



On the convexity of the Goldenblat–Kopnov yield condition

A. GANCZARSKI and J. LENCZOWSKI (KRAKÓW)

THE PRESENT PAPER is aimed at the formulation of sufficient conditions of convexity for the Goldenblat–Kopnov yield condition. The essence of the proposed approach consists in the transposition of convexity of hypersurface from the six-dimensional stress space to the three-dimensional space of the principal stresses, and in the presentation of a surface in the Haigh–Westergaard stress space.

1. Introduction

WHEN THE CLASSICAL FLOW THEORY of plasticity is used, the yield surface is often assumed to have the form of a potential representation, from which the strain rates are derived. The second Drucker stability postulate implies that the constitutive equations are always of the Green (hyperelastic) type. Hence, the strain energy and the complementary energy functions are always positive definite, whereas the corresponding surfaces defined in strain and stress spaces, respectively, are convex (see CHEN and HAN [3], also ŻYCKOWSKI [21]). For perfectly plastic materials, yielding itself implies failure, so the yield stress is also the limit strength. Therefore, for the failure surfaces a similar problem of convexity exists.

Obviously, the above requirements are also imposed on the flow theory of plastic anisotropic materials, as well as the anisotropic failure conditions.

2. The Goldenblat–Kopnov yield condition

Certain generalization of the Burzyński yield condition to the case of anisotropy has been proposed by GOLDENBLAT and KOPNOV [5]:

$$(2.1) \quad (\Pi_{ij}\sigma_{ij})^\alpha + (\Pi_{ijkl}\sigma_{ij}\sigma_{kl})^\beta + (\Pi_{ijklmn}\sigma_{ij}\sigma_{kl}\sigma_{mn})^\gamma + \dots = 1,$$

where α, β, γ are arbitrary numbers; nevertheless, only few combinations of them have a practical sense. When the most frequent case of $\alpha = \beta = 1, \gamma = 0$ is assumed, the yield condition (2.1) reduces to the Burzyński paraboloid yield condition (see ŻYCKOWSKI [21]):

$$(2.2) \quad \Pi_{ijkl}\sigma_{ij}\sigma_{kl} + \Pi_{ij}\sigma_{ij} = 1,$$

where the fourth-order tensor as well as the second-order tensor of plastic moduli satisfy the symmetry conditions $\Pi_{ijkl} = \Pi_{klij} = \Pi_{jikl} = \Pi_{ijlk}$, and $\Pi_{ij} = \Pi_{ji}$,

respectively. Consequently, 21+6 of such components are independent. In case of the orthogonal anisotropy (called orthotropy), a further reduction of the number of independent moduli is possible. Choosing the reference coordinate frame coinciding with the principal axes of orthotropy, the fourth-order tensor becomes independent of the mean stress and simultaneously, the second-order tensor becomes independent of the shear stresses (see THEOCARIS [19]). Moreover, 9 terms associated with normal and shear stress products, as well as products of two shear stresses of different indices vanish, and the following 9+3 terms remain:

$$(2.3) \quad \begin{aligned} & \Pi_{1111}\sigma_{11}^2 + \Pi_{2222}\sigma_{22}^2 + \Pi_{3333}\sigma_{33}^2 + 4\Pi_{1212}\sigma_{12}^2 + 4\Pi_{2323}\sigma_{23}^2 \\ & + 4\Pi_{3131}\sigma_{13}^2 + 2\Pi_{1122}\sigma_{11}\sigma_{22} + 2\Pi_{2233}\sigma_{22}\sigma_{33} + 2\Pi_{3311}\sigma_{33}\sigma_{11} \\ & + \Pi_{11}\sigma_{11} + \Pi_{22}\sigma_{22} + \Pi_{33}\sigma_{33} = 1. \end{aligned}$$

The material under consideration requires 9+3 tests: simple tension T_i , simple compression C_i along each axis of orthotropy, and simple shear Y_{ij} along each plane of orthotropy ($i, j = 1, 2, 3$); for orthotropic materials when the coordinate system coincides with the material symmetry directions, plastic shear stresses along reverse directions on the same plane do not differ: $Y_{ij}^+ = Y_{ij}^- = Y_{ij}$ (see THEOCARIS [19]). Replacing the index notation by the engineering notation, Eq.(2.3) takes more friendly form:

$$(2.4) \quad \begin{aligned} & a_1(\sigma_y - \sigma_z)^2 + a_2(\sigma_z - \sigma_x)^2 + a_3(\sigma_x - \sigma_y)^2 + a_4\tau_{yz}^2 + a_5\tau_{zx}^2 \\ & + a_6\tau_{xy}^2 + a_7\sigma_x + a_8\sigma_y + a_9\sigma_z = 1, \end{aligned}$$

where the new plastic moduli are defined as follows (see SOCHA and SZCZEPIŃSKI [18]):

$$(2.5) \quad \begin{aligned} a_1 &= \frac{1}{2} \left(\frac{1}{T_y C_y} + \frac{1}{T_z C_z} - \frac{1}{T_x C_x} \right), & a_2 &= \frac{1}{2} \left(\frac{1}{T_z C_z} + \frac{1}{T_x C_x} - \frac{1}{T_y C_y} \right), \\ a_3 &= \frac{1}{2} \left(\frac{1}{T_x C_x} + \frac{1}{T_y C_y} - \frac{1}{T_z C_z} \right), & a_4 &= \frac{1}{Y_{yz}^2}, & a_5 &= \frac{1}{Y_{zx}^2}, \\ a_6 &= \frac{1}{Y_{xy}^2}, & a_7 &= \frac{1}{T_x} - \frac{1}{C_x}, & a_8 &= \frac{1}{T_y} - \frac{1}{C_y}, & a_9 &= \frac{1}{T_z} - \frac{1}{C_z}. \end{aligned}$$

The plastic moduli a_1, a_2, \dots, a_9 are linear combinations of the components of fourth-order tensor Π_{ijkl} (see LEMAITRE and CHABOCHE [12], also MALININ and RZYSKO [14]) and second-order tensor Π_{ij} :

$$(2.6) \quad \begin{aligned} \Pi_{1111} &= a_1 + a_3, & \Pi_{2222} &= a_1 + a_2, & \Pi_{3333} &= a_2 + a_3, \\ \Pi_{1122} &= -a_1, & \Pi_{2233} &= -a_2, & \Pi_{3311} &= -a_3, \\ \Pi_{1212} &= a_4/4, & \Pi_{2323} &= a_5/4, & \Pi_{3131} &= a_6/4, \\ \Pi_{11} &= a_8, & \Pi_{22} &= a_9, & \Pi_{33} &= a_7. \end{aligned}$$

The function (2.4), being a special case of the yield condition presented by PARISEAU [15], can describe materials with different tensile and compressive strengths. RALSTON [16] employed Eq. (2.4) to crushing failure analysis of column-grained ice which exhibits orthotropy and sensitivity to hydrostatic pressure. However, if the yield stresses in tension are equal to that in compression (isosensitive material), $T_x = C_x = X$, $T_y = C_y = Y$, $T_z = C_z = Z$, the coefficients a_7, a_8, a_9 vanish, so the linear terms in Eq. (2.4) disappear:

$$(2.7) \quad a_1(\sigma_y - \sigma_z)^2 + a_2(\sigma_z - \sigma_x)^2 + a_3(\sigma_x - \sigma_y)^2 + a_4\tau_{yz}^2 + a_5\tau_{zx}^2 + a_6\tau_{xy}^2 = 1,$$

whereas the coefficients a_1, a_2, a_3 take the classical form of Hill's yield condition (see HILL [6] also JACKSON *et al.* [9]):

$$(2.8) \quad \begin{aligned} a_1 &= \frac{1}{2} \left(\frac{1}{Y^2} + \frac{1}{Z^2} - \frac{1}{X^2} \right), & a_2 &= \frac{1}{2} \left(\frac{1}{Z^2} + \frac{1}{X^2} - \frac{1}{Y^2} \right), \\ a_3 &= \frac{1}{2} \left(\frac{1}{X^2} + \frac{1}{Y^2} - \frac{1}{Z^2} \right). \end{aligned}$$

The classical Hill yield condition (2.7), consisting of the quadratic stress functions, that generalizes the Huber - Mises yield condition, has failed to account for the so-called "anomalous behaviour" of some commercial aluminum alloy and steel sheets. Therefore, a special case of the Hill generalized yield conditions has been developed (see HILL [7]):

$$(2.9) \quad a_1|\sigma_y - \sigma_z|^m + a_2|\sigma_z - \sigma_x|^m + a_3|\sigma_x - \sigma_y|^m + a_4|\tau_{yz}|^m + a_5|\tau_{zx}|^m + a_6|\tau_{xy}|^m = 1,$$

where the exponent m is equal to 6 or 8. The yield condition (2.9) is a generalization of the Hersey - Davis yield condition for $m = 2$ (and for $m = 4$), or the Tresca - Guest yield condition in the limiting case $m \rightarrow \infty$.

3. Convexity conditions

Although the yield function defined by Eq. (2.9) has been mathematically verified, and its convexity has been proved in case of the planar anisotropy in the principal stress space if and only if $m \geq 1$ and a_1, a_2, a_3, \dots are positive constant coefficients (see BARLAT and LIAN [1], also CHU [4]), in case of the general orthogonal anisotropy in the six-dimensional stress space and in the presence of terms associated with hydrostatic pressure, convexity of the yield surface (2.4) is not obvious.

Let us try to formulate convexity conditions for the yield functions (2.4) and (2.9). The yield condition (2.4) is defined in the six-dimensional stress space, and

if we can transform it to the three-dimensional space of the principal stresses, we will get rid of terms associated with second power of the shear stresses. However, it should be noted that for anisotropic materials, the yield condition is established in a certain reference coordinate system which is fixed with respect to the orientation of the material anisotropy. We cannot change the reference coordinate without changing the form of the yield condition. Moreover, the coefficients $a_1, a_2, a_3, \dots, a_9$ are not components of any tensor so they are not subjected to transformation rules of tensors. To avoid these inconveniences, first, we have to recover a tensor form of the yield condition expressing the coefficients $a_1, a_2, a_3, \dots, a_9$ by components of the fourth-order tensor Π'_{ijkl} and components of the second-order tensor Π'_{ij} of Eq. (2.6). Next, appropriate transformations from the directions of material orthotropy to the directions of principal stresses are done:

$$(3.1) \quad \Pi'_{ijkl} = \Pi_{mnrp} n_{im} n_{jn} n_{kr} n_{lp}, \quad \Pi'_{ij} = \Pi_{mn} n_{im} n_{jn},$$

where n_{ij} are direction cosines of the transformation.

Such a transformation is strictly associated with an important problem of the transposition of convexity from one space to another. SAYIR [17] proved such a transposition from the nine-dimensional stress space (in particular case, from the six-dimensional stress space) to the three-dimensional space of principal stresses, whereas LIPPMANN [13] from the three-dimensional space to the six-dimensional space.

When the new transformed coefficients $a'_1, a'_2, a'_3, \dots, a'_9$ are calculated from Π'_{ijkl} and Π'_{ij} by means of Eq. (2.6), the yield condition (2.4) referring to the principal stress axes takes a simplified form:

$$(3.2) \quad a'_1 (\sigma_1 - \sigma_2)^2 + a'_2 (\sigma_2 - \sigma_3)^2 + a'_3 (\sigma_3 - \sigma_1)^2 + a'_7 \sigma_3 + a'_8 \sigma_2 + a'_9 \sigma_1 = 1.$$

Last step is the geometric representation of the surface (3.2) in the Haigh–Westergaard stress space, where the three principal stresses ($\sigma_1, \sigma_2, \sigma_3$) are replaced by the Haigh–Westergaard coordinates (ξ, ϱ, θ) (see Appendix B):

$$(3.3) \quad \begin{Bmatrix} \sigma_1 \\ \sigma_2 \\ \sigma_3 \end{Bmatrix} = \frac{1}{\sqrt{3}} \begin{Bmatrix} \xi \\ \xi \\ \xi \end{Bmatrix} + \sqrt{\frac{2}{3}} \varrho \begin{Bmatrix} \cos \theta \\ \cos(\theta - 2\pi/3) \\ \cos(\theta + 2\pi/3) \end{Bmatrix}.$$

Substitution of (3.3) into (3.2) when the classical trigonometric identities are used, provides the formula for the surface radius:

$$(3.4) \quad \varrho(\theta, \xi) = \sqrt{\frac{2}{3}} \frac{\sqrt{B^2 + 12AC} - B}{4A},$$

where

$$(3.5) \quad \begin{aligned} A &= a'_1 \sin^2 \theta + a'_2 \sin^2(\theta + \pi/3) + a'_3 \sin^2(\theta - \pi/3), \\ B &= a'_7 \cos \theta + a'_8 \cos(\theta - 2\pi/3) + a'_9 \cos(\theta + 2\pi/3), \\ C &= 1 - \frac{\xi}{\sqrt{3}} (a'_7 + a'_8 + a'_9). \end{aligned}$$

In case of independence of the hydrostatic pressure of the generalized Hill yield condition (2.9) when $m \neq 2$, we have to set $A = \hat{A}$, $B = 0$, $C = 1$, and instead of Eq.(3.4), the surface radius is found from the formula

$$(3.6) \quad \begin{aligned} \varrho(\theta) &= \frac{1}{\sqrt{2}} \frac{1}{\sqrt[m]{\hat{A}}} \\ &= \frac{1}{\sqrt{2}} \frac{1}{\sqrt[m]{a'_1 \sin^m \theta + a'_2 \sin^m(\theta + \pi/3) + a'_3 \sin^m(\theta - \pi/3)}}. \end{aligned}$$

In case when the material isotropy ($a'_1 = a'_2 = a'_3 = 1/2\sigma_0^2$) and $m = 2$ are assumed, Eq.(3.6) reduces to the classical Huber - Mises yield condition:

$$(3.7) \quad \varrho = \sqrt{\frac{2}{3}} \sigma_0 = \text{const.}$$

Quadratic form containing linear terms of the yield condition (3.2) represents an *elliptic paraboloid* with a symmetry axis parallel to the hydrostatic axis, whereas the open end of the paraboloid is usually oriented towards the direction of hydrostatic compression (see THEOCARIS [19]). It is clear that only one of the coefficients a_1, a_2, a_3 in Eqs. (2.5) can be negative (see HILL [6]). Therefore, the loss of convexity consists in that an elliptic paraboloid may become at most an imaginary elliptic paraboloid, or in other words, a hyperbolic paraboloid. Consequently, the conditions of convexity of the yield surface are formulated as follows: the radius $\varrho(\theta, \xi)$ must be a real and positive number; Eqs. (3.4), (3.5) yield

$$(3.8) \quad \varrho(\theta, \xi) > 0 \quad \forall \theta, \xi,$$

and

$$(3.9) \quad \text{Im } \varrho = 0 \quad \Leftrightarrow \quad \xi \leq \frac{\sqrt{3}}{a'_7 + a'_8 + a'_9} \left(1 + \frac{B^2}{12A} \right).$$

In case of the generalized Hill yield surface, Eq.(3.6) represents an elliptical cylinder or at most a hyperbolic cylinder for which both conditions (3.8) and (3.9) ($\varrho(\theta) > 0 \quad \forall \theta$, and $\text{Im } \varrho = 0$) are equivalent to each other, and lead to the following inequality:

$$(3.10) \quad \hat{A} = a'_1 \sin^m \theta + a'_2 \sin^m(\theta + \pi/3) + a'_3 \sin^m(\theta - \pi/3) > 0, \quad \forall \theta.$$

4. Examples

4.1. Convexity of Hill's yield surfaces for the brass sheet L22

Most of anisotropic materials used in practice fulfil the convexity conditions (3.8) through (3.10), however there are few of them which do not.

Let us check convexity of the yield conditions which are independent of the hydrostatic pressure, namely (2.7) and its generalized form (2.9). MALININ and RZYSKO in [14] give plastic properties for a brass sheet of Russian commercial symbol L22, 0.8 mm thick: $\sigma_{0x} = X = 120$ MPa, $\sigma_{0y} = Y = 105$ MPa, $\sigma_{0z} = Z = 950$ MPa. Authors do not mention the shear yield stresses.

The difficulty in experimental defining the off-diagonal components of the fourth-order tensor resulted in a series of publications. Complicated tests were suggested, nevertheless they did not give the explicit form of the respective yield criterion. Therefore, several researchers used the simplifying assumption, when the small off-diagonal components (when compared to the diagonal ones) may be disregarded. This prediction, however, satisfactorily fits the experimental data only for two-dimensional loading models. On the other hand, off-axis biaxial tests indicate that vanishing of the off-diagonal components of the fourth-order tensor may lead to unreliable results.

Hence, the following *ad hoc* extensions of the classical definitions are introduced in the present paper: $\tau_{0ij} = Y_{ij} = \sqrt{\sigma_{0i}\sigma_{0j}/3}$ for $m = 2$, and $\tau_{0ij} = Y_{ij} = \sqrt{\sigma_{0i}\sigma_{0j}/2}$ for $m = 6, 8$. In case of material isotropy $\sigma_{0i} = \sigma_{0j} = \sigma_0$ we get values $\tau_0 = \sigma_0/\sqrt{3}$ (Huber - Mises) or $\tau_0 = \sigma_0/2$ (Tresca - Guest), respectively. Eventually, the complete material data are shown in Table 1.

Table 1. Yield stresses of brass L22 [14].

m	X [MPa]	Y [MPa]	Z [MPa]	Y_{zy} [MPa]	Y_{zx} [MPa]	Y_{xy} [MPa]
2	120	105	950	182	194	64.8
6 or 8	120	105	950	157	168	56.1

The Hill's yield condition (2.7) applied to the brass L22 represents an elliptic cylinder in the Haigh - Westergaard stress space. It turns out that semi-axes of the ellipse strongly depend on the direction cosines of the transformation Eq. (3.1). It has been seen from Table 1 that the direction of dominant material orthotropy is oriented parallel to the z axis of the coordinate system, whereas the plane xy exhibits slight orthotropy. Hence, the material is nearly transversely isotropic. Moreover, the material exhibits the group of symmetry which satisfies periodicity of at least one octant. Both coordinate systems associated with the directions of material orthotropy and the directions of principal stresses were linked, for convenience, by the Euler angles $(\varphi, \vartheta, \psi)$ (see Appendix A). The complete analysis

requires to check the yield condition versus all Euler angles in one octant, however it takes a lot of CPU time and memory. To avoid this inconvenience, the authors suggest to take advantage of the plane orthotropy mentioned above, and to check the yield condition for the pair of angles φ, ϑ ; the third angle ψ is not essential, and may be disregarded within the following range: $0 \leq \varphi \leq 90^\circ$ and $0 \leq \vartheta \leq 90^\circ$.

Let us follow the evolution of the yield condition in a simple case, when only one of the Euler angles, say ϑ , is subject to change, whereas two other are kept constant. When $\vartheta = 45^\circ$ we get the ellipse of moderate semi-axes ratio, about 1:3, each change of ϑ , either decrease or increase, increases this ratio. Consequently, the ellipse is subjected to rotation and, simultaneously, becomes, step by step, longer and more oblate. Finally, for $\vartheta = 0^\circ$ or $\vartheta = 90^\circ$, one of the semi-axes goes to infinity and the yield condition presents a hyperbolic cylinder (Fig. 1). As it was mentioned before, it is convenient to map the convexity of yield condition versus the pair of Euler angles: $0 \leq \varphi \leq 90^\circ$ and $0 \leq \vartheta \leq 90^\circ$, taken as a two-dimensional domain. The obtained map (Fig. 2) confirms the assumed group of the material symmetry; moreover, the higher-order symmetry of 45° versus angle φ is observed. The yield condition is convex in almost whole domain except for narrow zones around its corners.

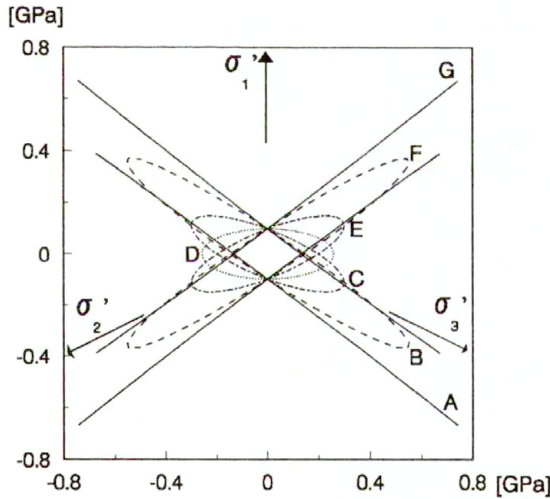


FIG. 1. Evolution of Hill's yield surface versus ϑ -Euler angle: A - 0° , B - 15° , C - 30° , D - 45° , E - 60° , F - 75° and G - 90° , for brass L22 [14].

In case of the generalized Hill yield condition (2.9) describing plastic behaviour of the brass L22, the yield surface ($m = 8$) is a prism of the semi-hexagonal cross-section with oval corners (Fig. 3). The loss of convexity resembles the previous case, each decrease or increase of ϑ versus the value 22° makes the hexagon more deformed until it becomes open.

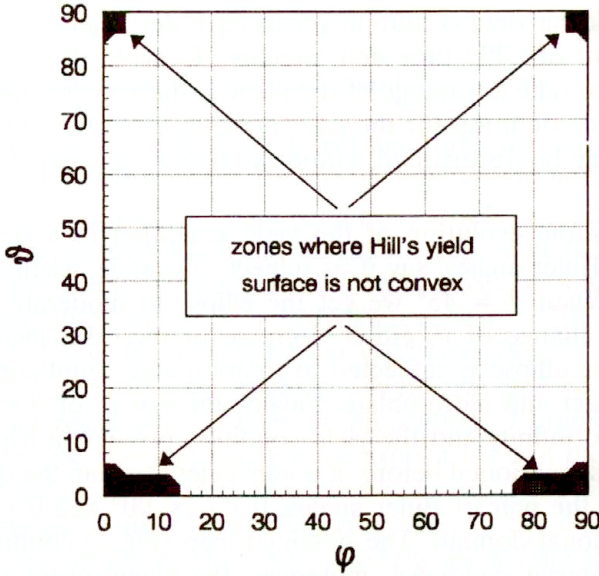


FIG. 2. Convexity map of Hill's yield surface versus φ, ϑ Euler angles for brass L22 [14].

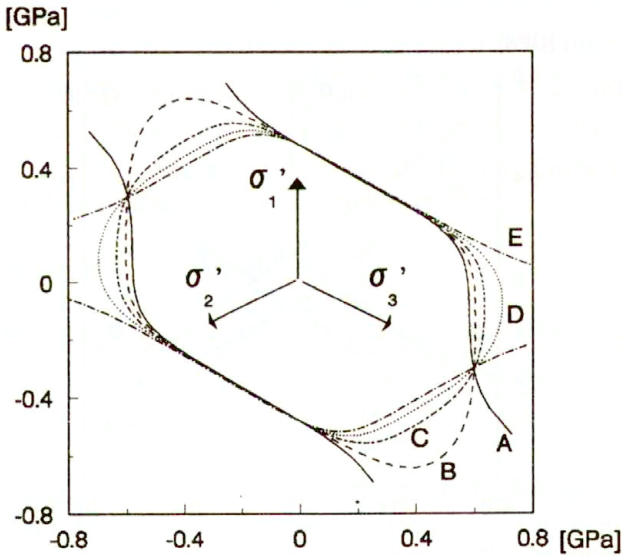


FIG. 3. Evolution of generalized Hill's yield surface ($m = 8$) versus ϑ -Euler angle: $A - 18^\circ, B - 20^\circ, C - 22^\circ, D - 24^\circ$ and $E - 26^\circ$, for brass L22 [14].

The convexity map is shown in Fig. 4. The area where the yield condition is convex has been significantly decreased when compared with the case $m = 2$ (see Fig. 2). Zones neighbouring the corners where the yield condition is not convex have increased significantly: two of them which refer to the angle $\vartheta = 0^\circ$ lie

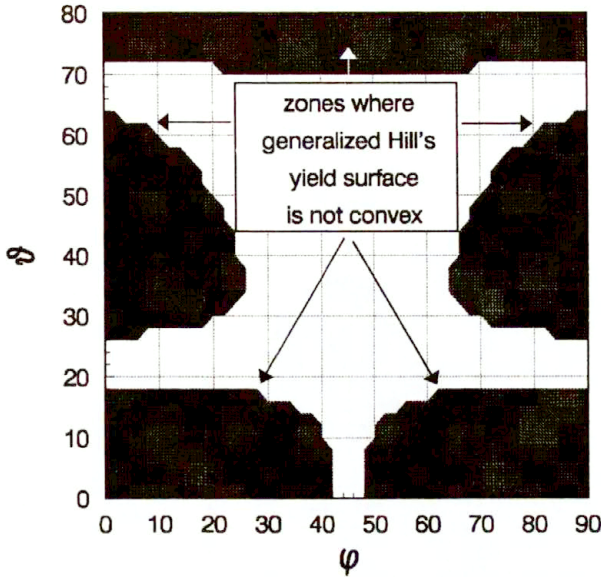


FIG. 4. Convexity map of generalized Hill's yield surface versus φ, ϑ Euler angles for brass L22 [14].

around the axis of symmetry $\varphi = 45^\circ$ and consequently, only a very narrow zone remains convex; moreover, two zones referring to the angle $\vartheta = 90^\circ$ have joined together and the yield condition has lost convexity in the whole range of φ . Two additional zones of nonconvexity, each of them oval in shape, have appeared for moderate values of $\vartheta = 45^\circ$.

4.2. Convexity of the Goldenblat–Kopnov yield surface (2.4) applied as failure criterion for the carbon woven roving-epoxy resin composite

Next example deals with checking the convexity of the function containing terms associated with the hydrostatic pressure (2.4), applied as the anisotropic failure condition of a composite. THEOCARIS [19] and WU [20] cite the experimental data for the composite with the reinforcement of a carbon *woven roving*, for which the material data are presented in Table 2⁽¹⁾.

Table 2. Anisotropic failure stresses of the carbon woven roving-epoxy resin composite [19, 20].

Failure stresses [MPa]								
T_x	C_x	T_y	C_y	T_z	C_z	Y_{yz}	Y_{zx}	Y_{xy}
1065.93	615.01	1065.93	615.01	42.40	143.20	21.20	21.20	532.96

⁽¹⁾ HOA [8] recommends to take Y_{ij} for woven roving as 0.5 of T_i . This value coincides with the tensile strength of woven roving tested at 45° .

The failure condition (2.4) used for the carbon woven roving-epoxy resin composite, for the Euler angles $\varphi = 45^\circ$, $\vartheta = 45^\circ$ forms an elliptic paraboloid, the axis of which coincides with the direction of the hydrostatic compression (Fig. 5). If we change φ or ϑ , the previously mentioned rotation of the ellipses and simultaneous loss of convexity of the surface is observed.

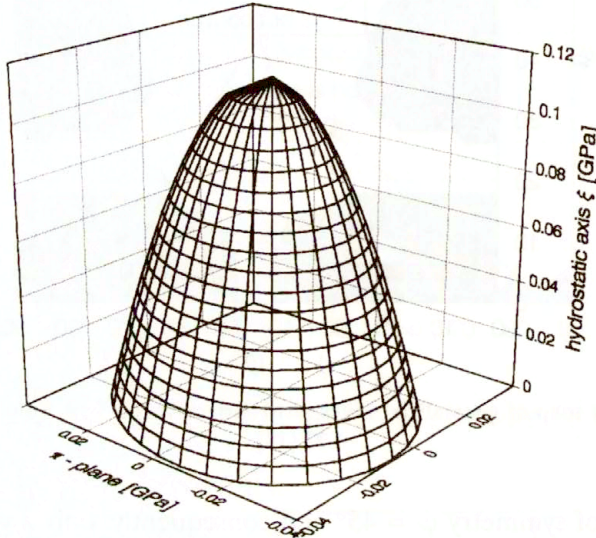


FIG. 5. The Goldenblat–Kopnov failure surface (Euler angles $\varphi = 45^\circ$, $\vartheta = 45^\circ$) for carbon woven roving-epoxy resin composite [19, 20].

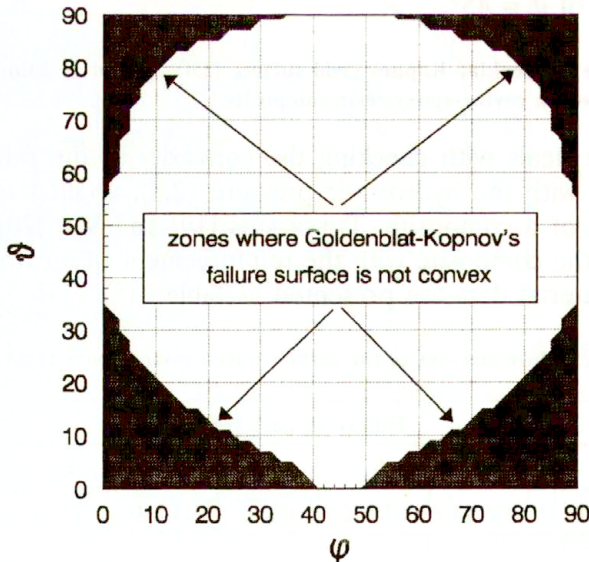


FIG. 6. Convexity map of Goldenblat–Kopnov failure surface versus φ , ϑ Euler angles for carbon woven roving-epoxy resin composite [19, 20].

Analyzing the map of convexity in Fig. 6, further reduction of area of convexity, due to anisotropy of the carbon woven roving-epoxy resin composite stronger than the brass L22, is observed. Zones of nonconvexity, around corners, have increased, and now reach almost $\vartheta = 35^\circ$ or $\vartheta = 55^\circ$, respectively. However, the central zone of oval shape guarantees convexity of the failure condition for all angles $\varphi \in \langle 10^\circ, 50^\circ \rangle$, $\vartheta \in \langle 10^\circ, 50^\circ \rangle$.

5. Conclusion

In the present paper, the convexity of the Goldenblat–Kopnov yield/failure criterion is analyzed. To illustrate the yield/failure surface in the Haigh–Wester-gaard stress space, the fourth-order Π_{ijkl} and the second-order Π_{ij} tensors of plastic moduli are transformed from the principal directions of material orthotropy to the principal stress directions. As examples of non-convex yield/failure conditions, included or not included hydrostatic pressure effect, a commercial brass sheet and a woven roving reinforced composite are chosen. A case of special interest is the dependence of convexity of a yield/failure surface on the direction cosines of transformation.

Appendix

A. Transformation of constitutive tensors to a new coordinate system

A tensor of rank four is subjected to the following rule of transformation:

$$(A.1) \quad T'_{ijkl} = T_{mnrp} l_{im} l_{jn} l_{kr} l_{lp},$$

whereas a tensor of rank two fulfills the appropriate transformation rule:

$$(A.2) \quad T'_{ij} = T_{mn} l_{im} l_{jn},$$

where for given i, j, k, l , the indices m, n, r, p are to be summed from 1 to 3. The formula (A.1) transforms the components of a tensor of rank four to new axes according to transformation rule, however an equivalent transformation is more convenient:

$$(A.3) \quad \hat{T}'_{ij} = \hat{T}_{mn} q_{im} q_{jn},$$

where actually indices m and n are to be summed from 1 to 6. In this way, a transformation of the fourth rank tensor T_{mnrp} is replaced by transformation of its representation matrix \hat{T}_{mn} , where symbols q_{ij} are taken from Table 3 (see LEKHNITSKII [11], also BATHE [2]).

Let us consider a convenient parametrization when a new coordinate system is obtained from the old one by rotation through Euler's angles. The following

Table 3. Symbols q_{ij} in transformation formulas.

i/j	1	2	3	4	5	6
1	l_{11}^2	l_{12}^2	l_{13}^2	$l_{12}l_{13}$	$l_{13}l_{11}$	$l_{12}l_{11}$
2	l_{21}^2	l_{22}^2	l_{23}^2	$l_{23}l_{22}$	$l_{23}l_{21}$	$l_{22}l_{21}$
3	l_{31}^2	l_{32}^2	l_{33}^2	$l_{33}l_{32}$	$l_{33}l_{31}$	$l_{32}l_{31}$
4	$2l_{31}l_{21}$	$2l_{32}l_{22}$	$2l_{33}l_{23}$	$l_{33}l_{22} + l_{32}l_{23}$	$l_{33}l_{21} + l_{31}l_{23}$	$l_{31}l_{22} + l_{32}l_{21}$
5	$2l_{31}l_{11}$	$2l_{32}l_{12}$	$2l_{33}l_{13}$	$l_{33}l_{12} + l_{32}l_{13}$	$l_{33}l_{11} + l_{31}l_{13}$	$l_{31}l_{12} + l_{32}l_{11}$
6	$2l_{21}l_{11}$	$2l_{12}l_{22}$	$2l_{13}l_{23}$	$l_{13}l_{22} + l_{12}l_{23}$	$l_{13}l_{21} + l_{11}l_{23}$	$l_{11}l_{22} + l_{12}l_{21}$

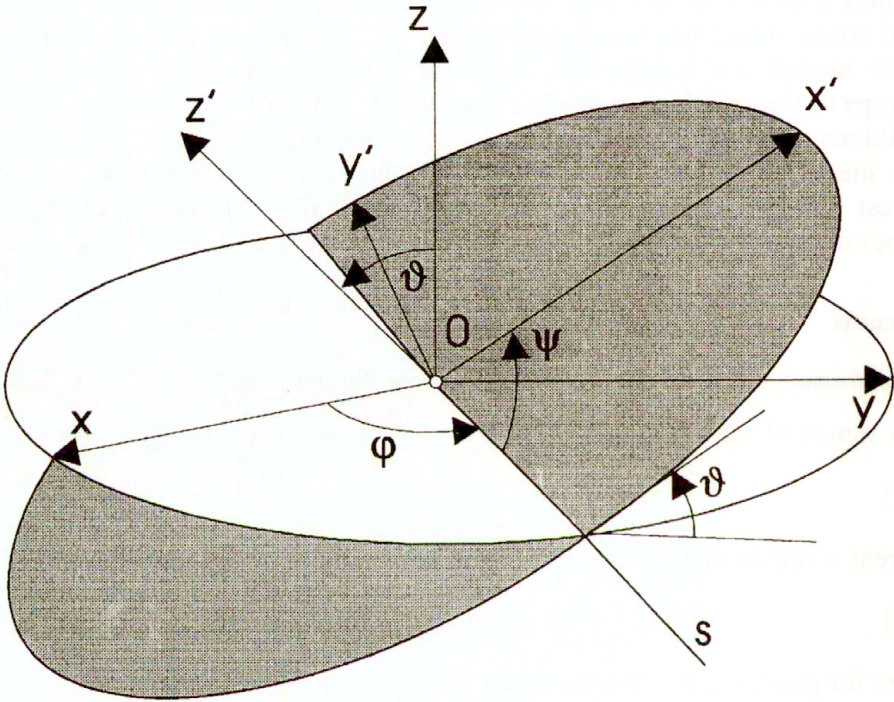


FIG. 7. The Euler angles.

sequence of rotations is taken into account (see Fig. 7); first rotation of the initial coordinate frame around z axis through precession angle ($0 \leq \varphi < 2\pi$), then rotation around the nodal line s through nutation angle ($0 \leq \vartheta \leq \pi$), and finally rotation around z' axis through angle ($0 \leq \psi < 2\pi$), for which the corresponding transformation matrices are as follows (see KARAŚKIEWICZ [10]):

$$(A.4) \quad \mathcal{A} = \begin{pmatrix} \cos \varphi & \sin \varphi & 0 \\ -\sin \varphi & \cos \varphi & 0 \\ 0 & 0 & 1 \end{pmatrix},$$

$$(A.4) \quad [cont.] \quad B = \begin{pmatrix} 1 & 0 & 0 \\ 0 & \cos \vartheta & \sin \vartheta \\ 0 & -\sin \vartheta & \cos \vartheta \end{pmatrix},$$

$$C = \begin{pmatrix} \cos \psi & \sin \psi & 0 \\ -\sin \psi & \cos \psi & 0 \\ 0 & 0 & 1 \end{pmatrix}.$$

Hence, the matrix of direction cosines takes the form:

$$(A.5) \quad l_{ij} = CBA.$$

In general case angles φ, ϑ, ψ are variable, but there are three basic cases. Namely, if angles φ and ϑ are constant, but angle ψ is variable, then the coordinate frame is subjected to rotation around the fixed axis z' . If angles ψ and ϑ are constant, but angle φ is variable, then the nodal line s is subjected to rotation around the axis z on plane xy , and simultaneously axis z' describes a cone around the z axis. If angles φ and ψ are constant, but angle ϑ is variable, then the nodal line s is fixed and plane $x'y'$ changes its inclination versus plane xy .

B. Haigh–Westergaard stress space

A very convenient representation of the stress state is the Haigh – Westergaard stress space which consists of the three principal stresses as coordinates.

Consider the straight line passing through the origin and equally inclined to the coordinate axes (see Fig. 8). Then for every point on this line, the state of stress fulfills the equality $\sigma_1 = \sigma_2 = \sigma_3$. In other words, every point on this line corresponds to a hydrostatic state of stress, this line is therefore named the hydrostatic axis. Furthermore, any plane perpendicular to the hydrostatic axis is called the deviatoric plane. Such a plane has the form:

$$(B.1) \quad \sigma_1 + \sigma_2 + \sigma_3 = \sqrt{3}\xi,$$

where ξ is the distance from the origin to the plane measured along the hydrostatic axis. The particular plane passing through the origin (for $\xi = 0$) is called the π -plane or the Meldahl plane.

An arbitrary state of stresses at a given point is decomposed into the hydrostatic and the deviatoric components, respectively:

$$(B.2) \quad (\sigma_1, \sigma_2, \sigma_3) = (1, 1, 1)\text{Tr}\sigma/3 + (s_1, s_2, s_3).$$

The vector representing the hydrostatic component $\xi = \text{Tr}\sigma/\sqrt{3}$ lies on the hydrostatic axis, whereas the vector representing the deviatoric component of length $\varrho = \sqrt{s_1s_2 + s_2s_3 + s_3s_1}$ lies on the deviatoric plane.

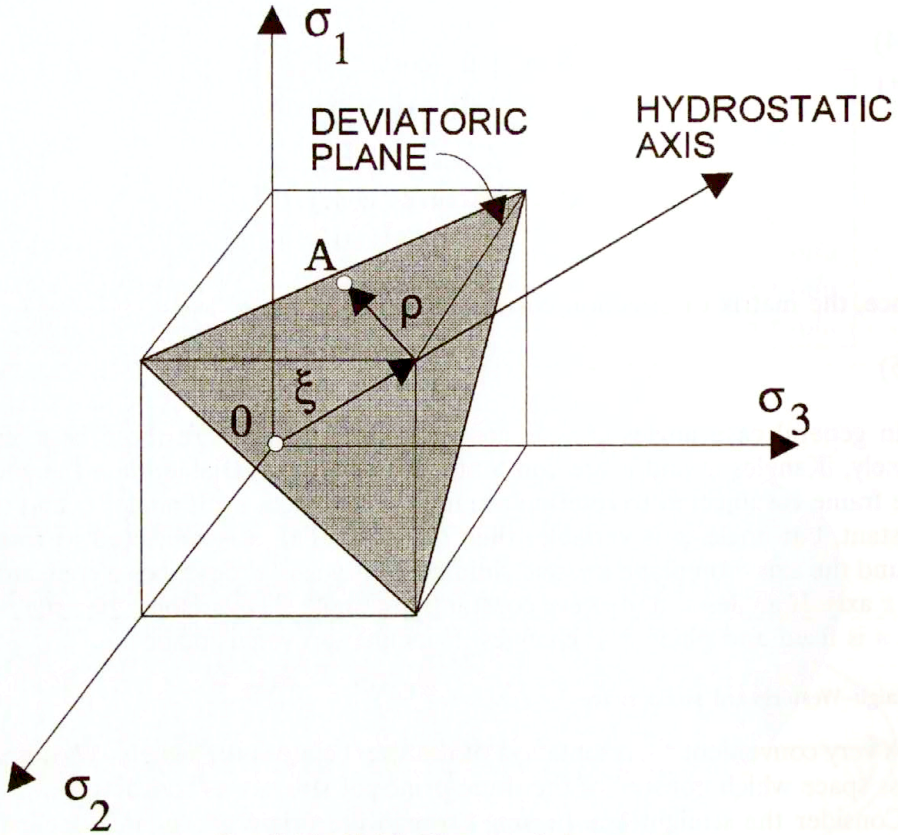


FIG. 8. The Haigh-Westergaard stress space.

Let us consider projections of both the deviatoric component and the coordinate axes on the π -plane (new and old unit vectors form the direction cosines equal to $\sqrt{2/3}$, hence new coordinates expressed in terms of the old ones are equal to $\sigma'_i = \sqrt{2/3}\sigma_i$):

$$(B.3) \quad \begin{aligned} s_1 &= \sqrt{\frac{2}{3}}\rho \cos \theta, & s_2 &= \sqrt{\frac{2}{3}}\rho \cos(2\pi/3 - \theta), \\ s_3 &= \sqrt{\frac{2}{3}}\rho \cos(2\pi/3 + \theta), \end{aligned}$$

where $0 \geq \theta \geq \pi/3$; then the state of stress $(\sigma_1, \sigma_2, \sigma_3)$ can be expressed by (ξ, ρ, θ) called the Haigh-Westergaard coordinates:

$$(B.4) \quad \begin{Bmatrix} \sigma_1 \\ \sigma_2 \\ \sigma_3 \end{Bmatrix} = \frac{1}{\sqrt{3}} \begin{Bmatrix} \xi \\ \xi \\ \xi \end{Bmatrix} + \sqrt{\frac{2}{3}}\rho \begin{Bmatrix} \cos \theta \\ \cos(\theta - 2\pi/3) \\ \cos(\theta + 2\pi/3) \end{Bmatrix}.$$

References

1. F. BARLAT and J. LIAN, *Plastic behavior and stretchability of sheet metals*, Int. J. Plasticity, **5**, 1, 51, 1989.
2. K.J. BATHE, *Finite element procedures in engineering analysis*, Prentice-Hall, Chapter 5, 258–259, 1982.
3. W.F. CHEN and D.J. HAN, *Plasticity for structural engineers*, Springer-Verlag, Chapter 2, 66–86, Chapter 3, 163–173, 1988.
4. E. CHU, *Generalization of Hill's 1979 anisotropic yield criteria*, Proc. NUMISHEET'89, 199–208, 1989.
5. I.I. GOLDENBLAT and V.A. KOPNOV, *A generalized theory of plastic flow of anisotropic metals* [in Russian], *Stroitel'naya Mekhanika*, 307–319, 1966.
6. R. HILL, *A theory of the yielding and plastic flow of anisotropic metals*, Proc. Roy. Soc., London, **A193**, 281–297, 1948.
7. R. HILL, *Theoretical plasticity of textured aggregates*, Proc. Camb. Phil. Soc., **85**, 179, 1979.
8. S.V. HOA, *Analysis for design of fiber-reinforced plastic vessels and pipings*, Techomic Publishing Co., Lancaster-Basel, Chapter 2, 48, 1991.
9. L.R. JACKSON, K.F. SMITH and W.T. LANKFORD, *Plastic flow in anisotropic sheet steel*, Metals Technology Techn. Publ., 2440, 1–15, 1948.
10. E. KARAŚKIEWICZ, *Introduction to theory of vectors and tensors* [in Polish], PWN, Chapter 1, 57–61, 1971.
11. S.G. LEKHNITSKII, *Theory of elasticity of an anisotropic body* [English transl.], Mir Publishers, Moscow, Chapter 1, 36–42, 1981.
12. J. LEMAITRE and J.L. CHABOCHE, *Mécanique des matériaux solides*, Bordas, Chapter 5, 184–187, 1985.
13. H. LIPPMANN, *Matrixungleichungen und die Konvexität der Fließfläche*, ZAMM, **50**, 1-4, 134–137, 1970.
14. N.N. MALININ and J. RZYSKO, *Mechanics of materials* [in Polish], PWN, Chapter 3, 119–155, 1981.
15. W.G. PARISEAU, *Plasticity theory for anisotropic rocks and solids*, Proc. 10th Symp. Rock Mech., Austin, Chapter 10, 1968.
16. T.D. RALSTON, *Yield and plastic deformation in ice crushing failure*, ICSI/AIDJEX Symp. Sea Ice-Processes and Models, Washington 1977.
17. M. SAYIR, *Zur Fließbedingungen der Plastizitätstheorie*, Ingenieur-Archiv., **39**, 6, 414–432, 1970.
18. G. SOCHA and W. SZCZEPIŃSKI, *On experimental determination of the coefficients of plastic anisotropy in sheet metals*, Arch. Mech., **46**, 177–190, 1994.
19. P.S. THEOCARIS, *Weighing failure tensor polynomial criteria for composites*, Int. J. Damage Mech., **1**, 4–46, 1992.
20. E.M. WU, *Mechanics of composite materials*, G.P. SENDECKYI [Ed.], Academic Press Publ., Chapter 9, 2, 353–431, 1979.
21. M. ŻYCZKOWSKI, *Combined loadings in the theory of plasticity*, PWN, Chapter 3, 94–126, 1981.

CRACOW UNIVERSITY OF TECHNOLOGY, KRAKÓW.

e-mail: artur@cut1.pk.edu.pl

Received November 8, 1996.